Copenhagen '12

P231

Anisotropic Migration Velocity Analysis Using the Elastic Wave Equation

W. Weibull* (Norwegian University of Science & Technology) & B. Arntsen (Norwegian University of Science & Technology)

SUMMARY

In this paper we investigate if elastic reverse time migration, combined with differential semblance optimization, can be used to estimate an anisotropic seismic velocity field. First we define formulas for elastic reverse time migration and for the differential semblance least squares misfit function. Next, we present the formulas for the gradient of the misfit function with respect to the velocities over a general anisotropic medium. Finally, we present two numerical examples that confirm the potential of the method both in estimating velocity parameters, and in improving depth imaging from synthetic surface seismic data.

Introduction

This paper deals with the problem of estimating anisotropic parameters for depth migration over a 2D transversely isotropic medium (TI) from surface seismic data. In an attempt to solve this problem, different methods have been proposed over the past few years (Zhou and Greenhalgh, 2008; Plessix and Rynja, 2010; Li and Biondi, 2011). In common, these methods are limited by strong approximations, and/or to a particular type of material symmetry (ex. VTI), which restricts their applicability. We propose a wave equation migration velocity analysis (WEMVA) method based upon elastic reverse time migration (ERTM). Because it uses the elastic two-way wave equation, the method can, in principle, deal with any physical form of material symmetry and wth any strength in the constrast of the material parameters. The method is an extension of the method for isotropic velocity analysis presented in Weibull and Arntsen (2011). The anisotropic parameters are estimated simultaneously through an iterative non-linear process aiming at minimizing the errors in the kinematics of the depth migrated images. In general, the velocity parameters can not be uniquely determined from surface seismic data alone due to the lack of sensitivity and/or ambiguity and tradeoff between the different parameters (Grechka et al., 2002). Nevertheless, our method can be used to generate a focused image of the subsurface that can be used as a frame to find better constrained and more unique solutions to the parameter estimation problem.

In the next section, we present the basic equations needed to set up and solve the optimization problem and then show two numerical examples which confirm the viability of the method on synthetic data.

Method and Theory

The theory for elastic reverse time migration is founded on non-linear inversion theory (Tarantola, 2005). Depth images are produced by crosscorrelating a source wavefield forward propagated in time with a residual wavefield backward extrapolated in time. In the context of elastic full waveform inversion, these images represent the gradients of the least square misfit function with respect to the material parameters. On the other hand, if the residual wavefield is given by the single scattering recorded data, we obtain Claerbout's imaging condition (Claerbout, 1971). According to this condition, given an accurate estimate of the material velocities, the crosscorrelation of the reconstructed source and receiver wavefields will have a maximum at zero lag in time and space. In Differential Semblance optimization we explore this fact to set up a non-linear least squares inversion problem (Symes and Carazzone, 1991). By parametrizing the image with an additional lag parameter we can capture the deviation of the maximum in crosscorrelation from zero lag, and use this to quantify the error in the estimates of the velocities.

In this paper we use an ERTM image (R) parametrized by horizontal spatial lag ($\mathbf{h}$):

$$R(\mathbf{x},\mathbf{h}) = \sum_s \int_0^T dt \; \frac{\partial u_i^{fw}}{\partial x_i}(\mathbf{x}-\mathbf{h},t,s)\frac{\partial u_j^{bw}}{\partial x_j}(\mathbf{x}+\mathbf{h},t,s), \tag{1}$$

with Einstein summation convention over i and j. The wavefields u_i^{fw} and u_i^{bw} are the reconstructed source and receiver wavefields, respectively. These wavefields are computed by solving the constant density elastic wave equation:

$$\begin{aligned} u_i^{fw}(\mathbf{x},t,s) &= \int d\mathbf{x}' \int_0^T dt \; G_{ij}(\mathbf{x},t;\mathbf{x}',0) \sum_{sou=1}^{Nsou} \delta(\mathbf{x}'-\mathbf{x}_{sou})\frac{\partial S}{\partial x_j}(\mathbf{x}_{sou},t,s) \\ u_i^{bw}(\mathbf{x},t,s) &= \int d\mathbf{x}' \int_0^T dt \; G_{ij}(\mathbf{x},0;\mathbf{x}',t) \sum_{rec=1}^{Nrec} \delta(\mathbf{x}'-\mathbf{x}_{rec})\frac{\partial P^{rec}}{\partial x_j}(\mathbf{x}_{rec},-t,s) \end{aligned}$$

Where G_{ij} is the constant density elastic Green's function, S is the pressure source function, P^{rec} is the recorded pressure data, $\mathbf{x} = (x_1, x_3)$ are the spatial coordinates, $\mathbf{h} = (h_1, 0)$ is the subsurface horizontal half-offset, t is the time and s is the source index.

The Differential Semblace misfit function quantifies the deviation from zero lag, and is given by (Weibull

and Arntsen, 2011):

$$DS = \frac{1}{2}\left\|\mathbf{h}\frac{\partial R}{\partial x_3}(\mathbf{x},\mathbf{h})\right\|^2 = \frac{1}{2}\int d\mathbf{x}\int d\mathbf{h}\,\mathbf{h}^2\left[\frac{\partial R}{\partial x_3}(\mathbf{x},\mathbf{h})\right]^2, \tag{2}$$

The errors quantified by the Differential Semblance misfit function can be turned into velocity updates by a non-linear iterative optimization process. In this process, it is necessary to compute the gradients of the misfit function with respect to the velocity parameters.

The gradients can be computed in a similar fashion to the depth migration described above, by the adjoint state method (Chavent, 2009):

$$\begin{aligned}\nabla_{\mathbf{m}} DS(\mathbf{x}) = &\sum_s \int dt \frac{\partial c_{ijkl}}{\partial \mathbf{m}}(\mathbf{x})\frac{\partial u_l^{fw}}{\partial x_k}(\mathbf{x},t,s)\frac{\partial \psi_i^{fw}}{\partial x_j}(\mathbf{x},t,s)\\ &+\sum_s \int dt \frac{\partial c_{ijkl}}{\partial \mathbf{m}}(\mathbf{x})\frac{\partial u_l^{bw}}{\partial x_k}(\mathbf{x},t,s)\frac{\partial \psi_i^{bw}}{\partial x_j}(\mathbf{x},t,s)\end{aligned} \tag{3}$$

Where c_{ijkl} is the elaticity tensor, and $\mathbf{m}$ depends on the velocity parametrization. In a 2D tranversely isotropic medium (TI), a possible choice of parametrization is given by $\mathbf{m} = [V_0(\mathbf{x}), \varepsilon(\mathbf{x}), \delta(\mathbf{x}), \theta(\mathbf{x})]$, where V_0 is the P-wave velocity along the symmetry axis, ε and δ are the Thomsen's parameters (Thomsen, 1986), and θ is the tilt angle of the symmetry axis. The wavefields ψ_i^{fw} and ψ_i^{bw} are adjoint states that can be computed by the following adjoint modelings:

$$\psi_i^{fw}(\mathbf{x},t,s) = \int d\mathbf{x}' \int_0^T \frac{\partial G_{ij}}{\partial x'_j}(\mathbf{x},0;\mathbf{x}',t)\int d\mathbf{h}\,\mathbf{h}^2\frac{\partial^2 R}{\partial x'^2_3}(\mathbf{x}'+\mathbf{h},\mathbf{h})\frac{\partial u_l^{bw}}{\partial x'_l}(\mathbf{x}'+\mathbf{2h},t)$$

$$\psi_i^{bw}(\mathbf{x},t,s) = \int d\mathbf{x}' \int_0^T \frac{\partial G_{ij}}{\partial x'_j}(\mathbf{x},t;\mathbf{x}',0)\int d\mathbf{h}\,\mathbf{h}^2\frac{\partial^2 R}{\partial x'^2_3}(\mathbf{x}'-\mathbf{h},\mathbf{h})\frac{\partial u_l^{fw}}{\partial x'_l}(\mathbf{x}'-\mathbf{2h},t)$$

Numerical examples

The first example in this section shows the behaviour of the Differential Semblance Misfit function for a simple TTI model. The model consists of a 1D layered model consisting of 3 layers with different values of the parameters V_0, ε, δ and θ, as shown in Figures 1A-C. We simulate surface seismic data over this model with a maximum offset of 1400 m. To generate the data we use a finite difference solution to the elastic wave equation (Lisitsa and Vishnevskiy, 2010). Perturbing the magnitude of parameters in the second layer and computing the Differential Semblance error, one at a time, allows us to plot a 1D curve showing the variation of the Differential Semblance misfit function for each parameter, as shown in Figures 1D-F. The major strength of this misfit function is that it is convex for a wide range of model perturbations, and therefore is particularly suitable for gradient based optimization. On the other hand, a major weakness of the misfit function, is that the optimum velocity is not the true one. This means that to converge to a very accurate solution, additional constraints must be placed or other more refined misfit functions must be used, such as the similarity-index (Chavent and Jacewitz, 1995; Zhou et al., 2009). The sensitivity of the Differential semblance misfit with respect to the different parameters is strongly dependent on the model and acquisition geometry (Grechka et al., 2002). The Figures 1D-F show that for the present example the objective function is most sensitive to V_0, and ε.

In the second example we show the results of a Differential Semblance Optimization over a VTI synthetic model of the Gullfaks field off the Norwegian Margin. We attempt to simultaneously obtain estimates for V_0, ε and δ. The initial model is an isotropic model where V_0 is a 1D model linearly increasing in depth from 1480 m/s to 3200 m/s. The data simulates a streamer data with minimum offset of 150m and maximum offset of 6km. The maximum frequency in the data is 30Hz. The results for the optimization after 20 iterations are pictured in Figure 2. The updated models show reasonable estimates of

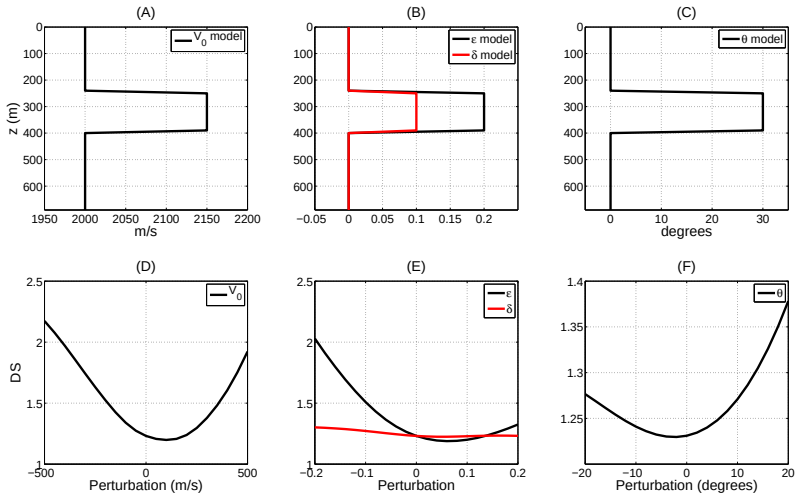

Figure 1 *A-C: 1D models used in example 1; D-F: Errors computed by perturbing the true models. Note that only one parameter is perturbed at a time, the other parameters are fixed at their true value.*

V_0, ε and δ, when compared to their true values. However, as can be seen from Figures 2B, 2C and 2D, the resolved parameters are strongly smoothed. This was a necessary constrain that helped reduce the null space and stabilize the optimization. Additionally, a bound contrained optimization was used so that the values of the anisotropy parameters could be constrained to have positive values. Figure 3A shows common image point gathers taken from position ($x = 2$ km) of the ERTM images constructed with the initial isotropic model (left), the optimized anisotropic model (centre) and the true set of parameters (right). These angle gathers, show that the updated model succeeds in improving the kinematics of the migrated image, in particular for the deeper events. For completeness, Figure 3B shows a comparison of logs of the different parameters for the same position ($x = 2$ km).

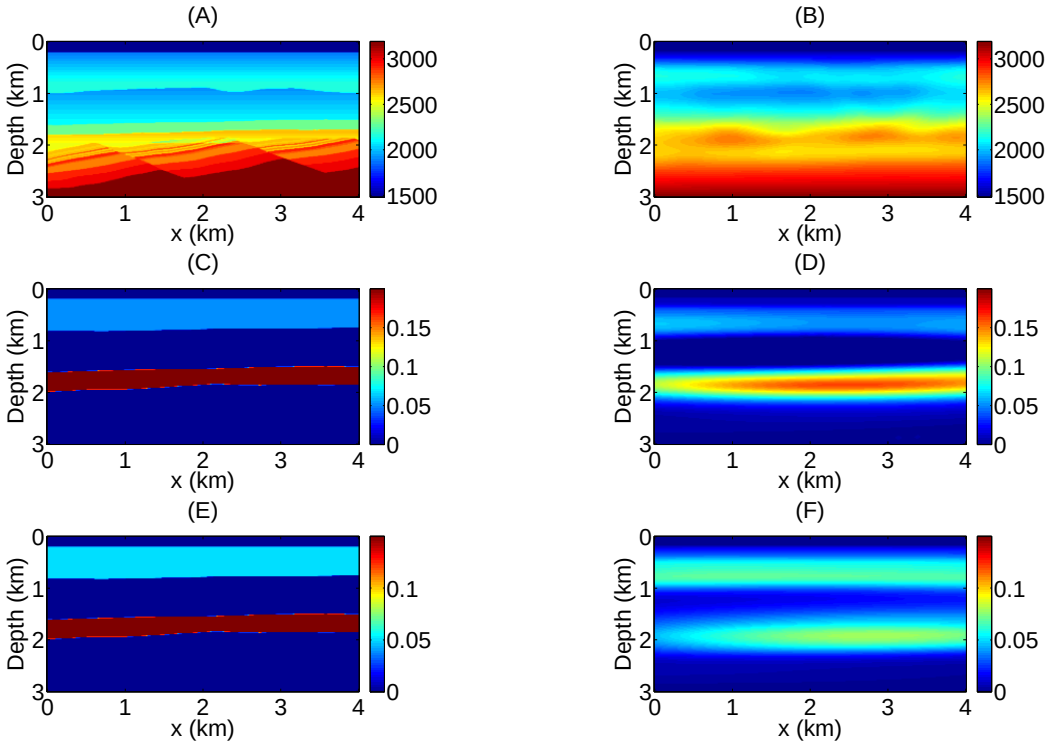

Figure 2 *A: True V_0 model; B: Updated V_o model; C: True ε model; D: Updated ε model; E: True δ model; F: Updated δ model.*

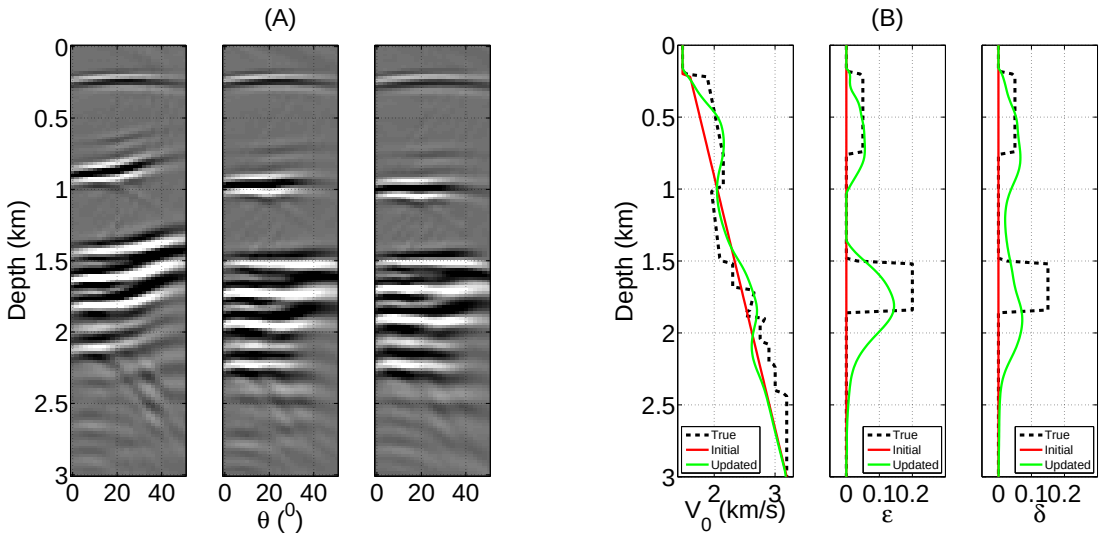

Figure 3 *A: Angle gathers at position ($x = 2$ km) - Initial (left), Updated (centre), True (Right); B: Comparison of velocity logs at position ($x = 2$ km) - V_0 (left), ε (centre), δ (Right).*

Conclusions

Anisotropic velocity models can be automatically estimated from surface seismic data by a non-linear optimization process based upon differential semblance and elastic reverse time migration. Through this process, the errors in the kinematics of migrated images are turned into parameter updates that help to improve the positioning of the reflectors in the depth migrated image. This can be explored to create better constrained models and mitigate the inherent non-uniqueness of the solution of this type of inverse problem.

Acknowledgements

The authors acknowledge the financial support of Statoil ASA and the sponsors of the ROSE consortium.

References

Chavent, G. and Jacewitz, C.A. [1995] Determination of background velocities by multiple migration fitting. *Geophysics*, **60**(02), 476–490.

Chavent, G. [2009] *Non-Linear Least Squares for Inverse Problems: Theoretical Foundations and Step-by-Step Guide for Applications*. Springer.

Claerbout, J.F. [1971] Toward a unified theory of reflector mapping. *Geophysics*, **36**(3), 467–481, doi: 10.1190/1.1440185.

Grechka, V., Pech, A. and Tsvankin, I. [2002] P-wave stacking-velocity tomography for VTI media. *Geophysical Prospecting*, **50**(2), 151–168, ISSN 1365-2478, doi:10.1046/j.1365-2478.2002.00307.x.

Li, Y. and Biondi, B. [2011] Migration velocity analysis for anisotropic models. *SEG San Antonio 2011 Anual Meeting*, Soc. of Expl. Geophys., 201–206.

Lisitsa, V. and Vishnevskiy, D. [2010] Lebedev scheme for the numerical simulation of wave propagation in 3d anisotropic elasticity. *Geophysical Prospecting*, **58**(4), 619–635, ISSN 1365-2478, doi:10.1111/j.1365-2478.2009.00862.x.

Plessix, R. and Rynja, H. [2010] VTI full waveform inversion: a parametrization study with a narrow azimuth streamer data example. *SEG Denver 2010 Anual Meeting*, Soc. of Expl. Geophys., 962–966.

Symes, W.W. and Carazzone, J.J. [1991] Velocity inversion by differential semblance optimization. *Geophysics*, **5**, 654–663.

Tarantola, A. [2005] *Inverse Problem Theory and Methods for Model Parameter Etimation*. SIAM (Society of Industrial and Applied Mathematics).

Thomsen, L. [1986] Weak elastic anisotropy. *Geophysics*, **51**(10), 1954–1966, doi:10.1190/1.1442051.

Weibull, W.W. and Arntsen, B. [2011] Reverse time migration velocity analsysis. *73th EAGE Conference & Exhibition*, European Association of Geoscientists and Engineers.

Zhou, B. and Greenhalgh, S. [2008] Non-linear traveltime inversion for 3-d seismic tomography in strongly anisotropic media. *Geophysical Journal International*, **172**(1), 383–394, ISSN 1365-246X, doi:10.1111/j.1365-246X.2007.03649.x.

Zhou, H., Liao, Q. and Ortigosa, F. [2009] Migration velocity inversion with semblance analysis (mVisa). *71st EAGE Conference & Exhibition*, European Association of Geoscientists and Engineers.